Advances in application of the limiting current technique for solid-liquid mass transfer investigations

J. Zalucky[†], S.S. Rabha[†], M. Schubert[†], U. Hampel[†,‡], Helmholtz-Zentrum Dresden-Rossendorf, Dresden, Germany*

[†]Institute of Fluid Dynamics, Helmholtz-Zentrum Dresden-Rossendorf, Bautzner Landstraße 400, 01328 Dresden, Germany

[‡]AREVA Endowed Chair of Imaging Techniques in Energy and Process Engineering, Technische Universität Dresden, 01062

*Corresponding author. Email: m.schubert@hzdr.de

This work was originally published and printed as part of the proceedings for the conference "2nd International Symposium on Multiscale Multiphase Process Engineering" taking place in Hamburg (Germany) during September 24-27, 2014.

The work may be cited as follows:

> Zalucky, J.; Rabha, S. S.; Schubert, M.; Hampel, U. Advances in application of the limiting current technique for solid-liquid mass transfer investigations. *2nd Internat. Symposium on Multiscale Multiphase Process Engineering, September 24-27, Hamburg, Germany* **2014**.

Advances in application of the limiting current technique for solid-liquid mass transfer investigations

J. Zalucky, S.S. Rabha, M. Schubert, U. Hampel, Helmholtz-Zentrum Dresden-Rossendorf, Dresden, Germany

ABSTRACT

The limiting current technique has widely been used to study liquid-solid mass transfer in various reactor configurations. In the present contribution several underlying physical aspects have been investigated in order to improve the design of mass transfer experiments. Experimentally, the significant influence of electrolyte composition and hydrodynamic conditions have been studied and quantified to ensure conditions of high reproducibility. In the course of single phase COMSOL simulations, different electrode configurations have been examined with emphasis on concentration fields and electric current distribution showing a large sensitivity of the experimental configuration on the absolute current values.

KEY WORDS
Liquid-solid mass transfer, limiting current technique, electric field simulation, ceramic solid foams

1. Introduction

In catalytic multiphase reactors, such as trickle-bed reactors, the achievable space-time yield strongly depends on the individual mass transfer steps. As the liquid-sold mass transfer (LSMT) to and from the solid surface is a resistance to all reactants, it denotes a very crucial parameter [1] to the over-all reactor efficiency. A common tool to quantify LSMT is the limiting current technique, which has been often presented in the literature since the 1960's [2]. In contrast to the dissolution techniques it implies the application of an electric potential to metal electrodes (mostly nickel) of a morphology representative for the packing.
In the present case, the focus is on highly tortuous open-cell solid foams made of silicon-infiltrated silicon-carbide (SiSiC). Showing an exceptional combination of high specific surface area and thermal conductivity as well as comparably low pressure drop, these structures have gained great interest as catalyst support in recent years. On the contrary, the investigation of liquid solid mass transfer in solid foam structures is currently scarce [3]. However, before applying the limiting current technique to these structures, a more detailed design of experiment is required concerning electrode design, alignment and electrode cleaning procedures. An extensive literature review disclosed substantial knowledge gaps about the underlying physical processes affecting the results of experiments.
In the present contribution, the most critical aspects, namely the effects of electrode surface area and area ratios, electrode distance and cleaning procedures, will be studied by the use of stirred-tank experiments and COMSOL simulations.

2. Limiting current technique

The limiting current technique was for the first time described by Eisenberg et al. [4] and can be described as follows:
When applying a potential to two electrodes in

an electrolyte solution, the corresponding ion flux can be determined by measuring the electric current. Depending on the applied voltage over fixed electrodes surrounded by an appropriate electrolyte, three regions can be identified (from low to high potentials):
It starts with the kinetic region (region I in **Fig. 1**), where the electrode kinetics of the limiting ion rules the occurring current. With rising potential the current curve levels to a plateau denoting the limiting current before rising again at higher potentials due to occurring secondary reactions.

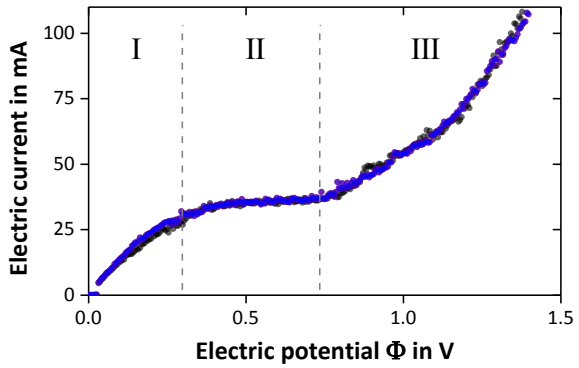

Fig. 1: Representative current over applied potential plot with regions dominated by kinetics (I), mass-transfer limitation (II) and secondary reactions (III).

In region II the plateau reflects the potential region, where the mass transfer of the limiting ion restricts the electrode reaction and is given by

$$I_{\mathrm{lim}} = \dot{n} \cdot z \cdot F \tag{1}$$

with

$$\dot{n} = k_{\mathrm{LS}} \cdot A \cdot (c_{\mathrm{bulk}} - c_{\mathrm{surf}}) \tag{2}$$

With the assumption of negligible small surface concentration, c_{surf}, the mass transfer can be calculated as:

$$k_{\mathrm{LS}} \cdot A = \frac{I_{\mathrm{lim}}}{z \cdot F \cdot c_{\mathrm{bulk}}} \tag{3}$$

Mostly, the limiting current technique is carried out by using the redox reaction of potassium hexacyanoferrit ($K_3Fe(CN)_6$) and potassium hexacyanoferrate ($K_4Fe(CN)_6$) in an aqueous solution. In order to suppress migration induced mass transfer [2], potassium carbonate [5] or sodium hydroxide [6] are commonly added as support electrolyte.

In the next section, the experimental approach and the results of the stirred-tank experiments will be discussed. In the second part, the COMSOL simulation results will be presented.

3. Stirred tank experiments

In order to study the reaction kinetics, the extent and time of both the electrolyte decay and the electrode surface de-activation, stirred-tank experiments were carried out in a double-walled glass beaker under isotherm operating conditions. Mass-transfer limitation was avoided by intensive mixing with a blade stirrer operated with up to 1600 rpm. A single nickel sphere and a nickel sheet, each soldered to a nickel wire and fixed to the beaker lid, were used as working and reference electrode, respectively. The application of the potential and the current measurement were realized by the use of a Meinzberger PS 2000 potentiostat. All experiments were carried out in nitrogen atmosphere without light access. The electrolyte solution was renewed each day. The solution composition and the operating conditions are given in **Table 1**.

Table 1: Operation parameters of the stirred tank experiments. Underlined values are considered as “reference” conditions.

Parameter	Value	Unit
Electrode potential	0.0 - 0.3	V
Concentrations		
$K_3Fe(CN)_6$	<u>0.01</u>	mol·L^{-1}
$K_4Fe(CN)_6$	0.01, <u>0.03</u>, 0.05	mol·L^{-1}
Na_2CO_3	0.5, <u>1.0</u>, 2.0	mol·L^{-1}
Stirrer speed	1000, 1200, <u>1600</u>	rpm
Temperature	<u>25</u>, 30, 35, 40	°C
Electrode geometry		
Sphere (WE)	Ø3	mm
Sheet (RE)	10 x 35 x 0.3	mm³

As support electrolyte, sodium carbonate was chosen, which has been reported superior to hydroxide based solutions by Szanto et al. [7]. Prior to each measurement set, beaker, electrodes and stirrer were carefully cleaned twice with deionized water. Between the experiments the electrodes were stored in deionized water. A set of experiments at one solution composition consisted of twelve experimental points (three stirrer speeds x four

temperatures) plus one reference experiment (lowest temperature, highest stirrer speed). Each current curve (for potentials ranging from 0 to 300 mV) was measured twice. Electric potentials over 300 mV were not applied in order to avoid the formation of unwanted ion species. The kinetic current was considered by averaging the current at 50 mV electric potential, which is considered as the kinetic region with negligible hydrodynamic influences.

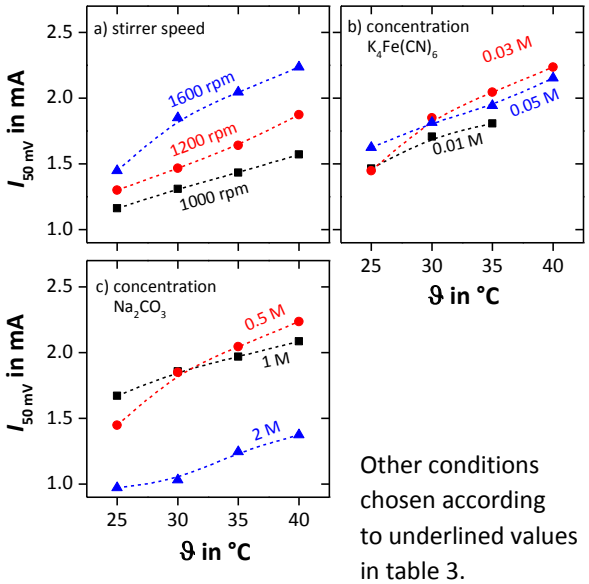

Other conditions chosen according to underlined values in table 3.

Fig. 2: Average electric current at 50 mV potential with a) stirrer speed, b) $K_4Fe(CN)_6$ and c) support electrolyte concentration varied.

The experiments revealed that the term '*kinetic*' might not be correct, as the current values constantly rise with the stirrer speed over the whole range of temperatures (**Fig. 2a**).
In addition, the amount of the non-limiting component $K_4(FeCN)_6$ has also an influence on the achieved current leading to deviations of 1% to 12% (**Fig. 2b**). The concentration of the support electrolyte (**Fig. 2c**), however, has only moderate influence for low concentrations (around 8% deviation), but detrimental effect when its concentration is increased (up to 44% relative loss). According to Berger and Ziai [8], this can be explained by the increasing Schmidt number due to increased density and viscosity of the liquid altering the flow conditions and ion diffusivities.
Concerning the daily reference experiments (**Fig. 3**), deviations of 1% to 5% were encountered. Yet, this might also trace back to slightly deviating flow conditions between the references and is within an acceptable range.

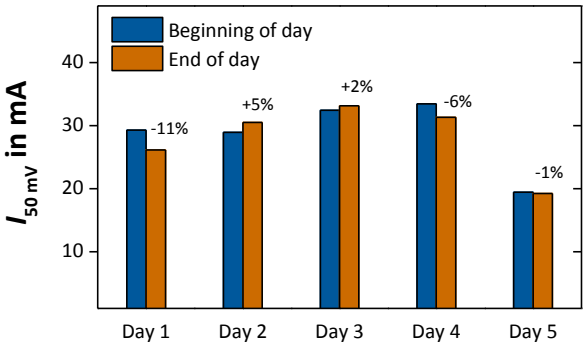

Fig. 3: Average electric current at 50 mV potential at chosen reference points achieved with different daily electrolyte compositions.

Ultimately, the limiting current technique could be considered as a fairly reproducible mass transfer measurement technique on the one hand. On the other hand, the strong influence of electrolyte composition on the electric current of up to 44% due to different operation parameters indicates a rather low comparability of results between different setups, which will also be discussed further based on the performed simulations.

4. Two-dimensional single phase COMSOL simulation

In order to understand the physics of the limiting current technique, a two-dimensional single phase flow model has been implemented in COMSOL 4.3b. By using the physics modules Laminar Flow (spf), Electrostatics (es), Transport of Diluted Species (chds) and Secondary Current Distribution (siec), the current-induced surface reaction of the above mentioned redox system has been modelled. As commonly done in experiments mentioned in the literature [6], the redox electrolytes are added in non-equimolar concentration in order to ensure concentration limitations of $K_3Fe(CN)_6$ at the working electrode.
The geometry consists of 21 stacked rows of equally distributed spheres of 4 mm diameter in a cross-section of 120 mm height and 50 mm width, which is flown through by single phase laminar flow from top to bottom.
Different electrode configurations were coupled together in order to study the influence of electrode distance, area ratios and alignments. In accordance to configurations in the literature,

axial and radial aligned integral (configurations A and B) and single sphere (configurations C and D) electrodes were investigated as shown in **Fig. 4.**

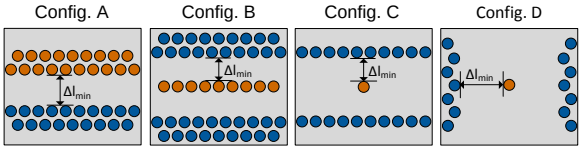

Fig. 4: Simplified scheme of working (orange) and reference (blue) electrode configurations studied with COMSOL.

The amounts and alignments of the coupled electrode spheres are described in **Table 2**. Additional simulation parameters are given in **Table 3**.

Table 2: Number and alignment of spheres in studied different configurations.

Configur-ation	Working electrode	Reference electrode	Alignment
A1	57	57	single stack
A2	10+9	10+9	single stack
B	9	2x (10+9)	sandwich
C	1	2x 9	sandwich
D	1	2x 9	radial

Table 3: Additional simulation parameters.

Parameter	Value	Unit
Electrode potential	0.2	V
Inlet concentration		
$K_3Fe(CN)_6$	0.01	$mol \cdot L^{-1}$
$K_4Fe(CN)_6$	0.03	$mol \cdot L^{-1}$
Laminar inlet velocity	0.05	$m \cdot s^{-1}$

One of the most important aspects to study is the concentration field around the electrodes, which can be seen in **Fig. 5** for the case A1. Around the working electrode, the concentration of the limiting component $K_3Fe(CN)_6$ decreases as expected before increasing slightly again, when passing the reference electrode (RE). Yet, the concentration field distribution differs from a conventional catalyst bed where the reaction rate depends only on the local concentrations. In the present case, the reaction rate seems to depend on the individual sphere position in its electrode group.

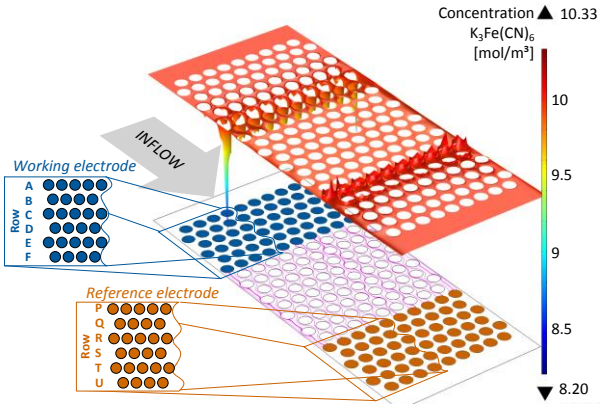

Fig. 5: COMSOL plot of the rate-limiting $K_3Fe(CN)_6$ concentration and the electric field. Electrode configuration A1 with working electrode sphere rows A to F (blue) and RE sphere rows P to U (orange).

When analyzing the electric field and the distribution of the electric current around the working electrode sphere rows A to F, a strong position-dependent distribution of the currents has been encountered, which is depicted in **Fig. 6**. Though six rows (rows A to F in **Fig. 5**) were electrically connected as nickel electrodes in the simulation, about 99.7% of the achieved total electric current flows through the three lower rows (D to F) of the working electrode. In accordance to the principle of electric currents using the path of least resistance, almost 75% of the flux passes through the electrode row closest to the reference electrode (and vice versa for the reference electrode).

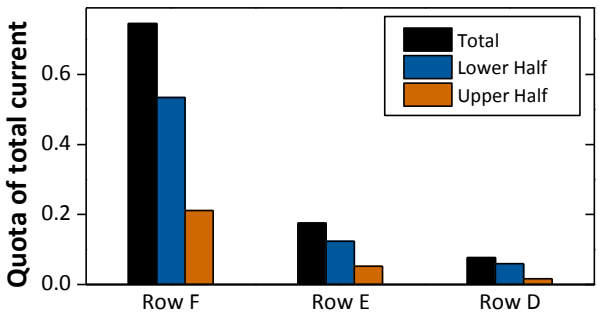

Fig. 6: Total current distribution over rows D to F.

Conclusively, a working electrode consisting of three rows yields the same conversion compared with a working electrode with more rows. Moreover, the lower hemispheres always contributed more to the electric flux than the upper halves as latter ones are shaded from the electric field. Physically, both effects result from the penetration depth of the electric field in

non-planar electrodes as studied for example by Winsel [9]. Furthermore, different electrode configurations described above were simulated in order to study effects contributing to the current and therefore to the mass-transfer rates reported in literature.

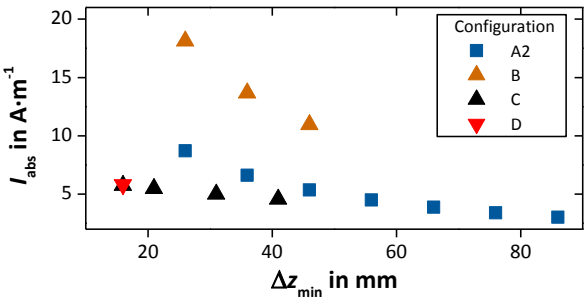

Fig. 7: Absolute electric current flux over minimal electrode distance for different working electrode configurations.

According to the simulated electric current (**Fig. 7**), the optimized sandwich stack configuration B yields the highest total current flux and conversion, but is affected strongest by the influence of the electrode distance.

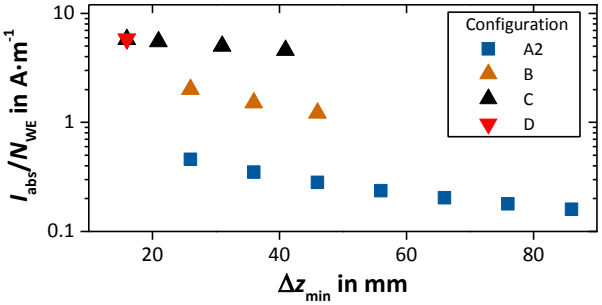

Fig. 8: Sphere count normalized electric current flux over minimal electrode distance for different working electrode configurations.

However, when normalizing the current, I, to the involved working electrode sphere count, N_{WE}, the single sphere configurations C and D at comparable electrode distances exceed configurations A and B by a factor of 16 and 2.8, respectively,. In the simulations, the configurations C and D differ only slightly as a) mass-transfer limitation effects were not foreseen in the simulation and b) surface discrimination was not yet fine enough.

Nevertheless, from the above results several conclusion can be drawn for the an optimal experimental design:

i. Packing electrodes shall not exceed a certain thickness as the shaded side opposite to the counter-electrode will not contribute to the conversion.
ii. Local, single-sphere experiments (config. C or D) cannot be directly compared to integral, multi-sphere configurations (config. A or B) as the resulting current densities and conversions differ tremendously.
iii. In order to avoid misrepresentation by electric shading effects, sandwich configurations comparable to config. B should be preferred for integral measurements.
iv. Mass transfer coefficients k_{LS} of composed electrodes should be considered with care as the electrode area A participating in the reaction is unknown in most cases.
v. Comparisons of $k_{LS}A$ or $\phi\, k_{LS}A$ of different experimental setups may differ largely due to electrode distance effects. However, comparisons of different flow conditions in one setup might be reasonable.
vi. Experiments in radial (config. D) and axial (config. C) electrode alignments will yield in different results due to different contributions of the working electrode circumference.

5. Conclusion

In the present contribution, several aspects of the limiting current technique have been discussed, which will affect mass transfer investigations in any setup. In the experiments, electrolyte composition and stirrer speed were found to affect the measured electric currents even in the so-called kinetic regime contrary to theoretical considerations. The reproducibility of the experiments, however, was between 1% to 5% deviations. With the simulations a strong dependency of the currents on the electrode configuration was shown. Finally, the limiting current technique proved to be fairly reproducible technique, which strongly depends on diverse experimental parameters making direct comparisons between different setups rather difficult.

Acknowledgment

This work was funded by the Helmholtz

Association within the frame of the Helmholtz Energy Alliance "Energy Efficient Chemical Multiphase Processes".

REFERENCES

[1] J. Battista, U. Böhm, Chem. Engin. Tech., 2003, 26, 1061–1067, DOI: 10.1002/ceat.200301739.

[2] J. Trueb, Disseration, 1960.

[3] I. Mohammed, T. Bauer, M. Schubert, R. Lange, Chem. Eng. Sci., 2014, 108, 223–232, DOI: 10.1016/j.ces.2013.12.016.

[4] M. Eisenberg, C. W. Tobias, C. R. Wilke, J. Electrochem. Soc., 1954, 101(6), 306–320, DOI: 10.1149/1.2781252.

[5] A. Burghardt, G. Bartelmus, M. Jaroszynski, A. Kolodziej, Chem. Eng. J., 1995, 58, 83–99, DOI: 10.1016/0923-0467(94)02956-3.

[6] R. Joubert, W. Nicol, The Canadian Journal of Chemical Engineering, 2012, 91, 441–447, DOI: 10.1002/cjce.21668.

[7] D. A. Szanto, S. Cleghorn, C. Ponce-de-Leon, F. C. Walsh, AIChE Journal, 2008, 54, 802–811, DOI: 10.1002/aic.11420.

[8] F. P. Berger, A. Ziai, Chemical Engineering Research and Design, 1983, 377–382.

[9] A. Winsel, Chem.-Ing.-Tech., 1971, 43, 191–195, DOI: 10.1002/cite.330430415.